Interplay between lead carboxylate and Ti or Zr isopropoxides in solution routes to perovskites: synthesis, molecular structures and reactivity of single source non-oxo Pb–Zr and Pb–Ti carboxylatoalkoxides supported by 2-ethylhexanoate ligands

Anne Brethon,[a] Liliane G. Hubert-Pfalzgraf*[a] and Jean-Claude Daran[b]

Received 15th September 2005, Accepted 14th October 2005
First published as an Advance Article on the web 3rd November 2005
DOI: 10.1039/b513142c

The reactions between $Ti(O^iPr)_4$ and $Zr_2(O^iPr)_8(HO^iPr)_2$, respectively, and lead 2-ethylhexanoate $Pb(O_2CC_7H_{15})_2$ have been investigated at rt and by heating. The initial mixed-metal species, characterized by single-crystal X-Ray diffraction, were adducts namely $Pb_4Zr_4(\mu\text{-}O_2CR')_8(\mu\text{-}OR)_6(\mu_3\text{-}OR)_2(OR)_8(OHR)_2$ **1** and $Pb_2Ti_4(\mu\text{-}O_2CR')_4(\mu\text{-}OR)_6(\mu_3\text{-}OR)_2(OR)_8$ **2** ($R' = CHCH(Et)C_2H_4Me$, $R = {}^iPr$) independently of the stoichiometry used. They are the first Pb–Ti and Pb–Zr non-oxo carboxylatoalkoxides reported. **1** is also the first Pb–Zr species based on an alkoxide-carboxylate ligand set matching the $PbZrO_3$ stoichiometry. Both structures are centrosymmetric with six-coordinate transition metals, as required for the perovskite, and are based on triangular M_2Pb cores (M = Zr, Ti). The lead centers display quite high coordination numbers, six and seven. The thermal and hydrolytic condensation reactions of **1** and **2** were investigated. Heat treatment of **2** and elimination of the volatiles under vacuum afforded $Pb_2Ti_3(\mu_4\text{-}O)(\mu_3\text{-}O)(\mu\text{-}O_2CC_7H_{15})_2(\mu\text{-}O^iPr)_6(O^iPr)_4$ **3** resulting from extrusion of $Ti(O^iPr)_4$ and scrambling of carboxylate ligands. Characterization of the various compounds was achieved by elemental analysis, FT-IR, ^1H and ^{207}Pb NMR.

Introduction

The $PbZr_xTi_{1-x}O_3$ (PZT) ceramic remains one of the most studied ferroelectric due to the diversity of its applications, actuators, sensors, piezoelectric devices to name but a few.[1] Chemical routes such as MOCVD (Metal Organic Chemical Vapour Deposition),[2] sol–gel processing[3] or MOD (Metal Organic Deposition)[4] have been used for access to coatings. The usual solution routes are based on easily accessible lead carboxylates and metal alkoxides using various solvents and/or additives such as diols or β-diketones for instance for improving stability or allowing patterning.[5] Lead acetate and/or its hydrate was thus often associated to various alkoxides in 2-methoxyethanol.[3] Long-chain carboxylates such as 2-ethylhexanoates are the choice precursors for MOD.[4] Reactions between lead 2-ethylhexanoate and *n*-butoxides of group 4 metals are a system of easy commercial access which has the advantage to avoid the drawback of the use of 2-methoxyethanol.[6] Reproducibility for industrial processes requires the use of solutions with a minimum of preparation as well as a better understanding of relationships between structure–processing–properties. Structurally characterized mixed-metal Pb–Ti and Pb–Zr heterometallics are generally based on ethoxide or isopropoxide- and acetate ligand sets.[1b,7] Typical compounds are $Pb_2Ti_4(\mu\text{-}O)_2(\mu\text{-}OAc)_2(OEt)_{14}$[8] and $Pb_2Zr_4(\mu\text{-}O)_2(\mu\text{-}OAc)_4(OEt)_{12}$[9] for the ethoxide but $Pb_2Ti_2(\mu_4\text{-}O)(\mu\text{-}OAc)_2(O^iPr)_8$ and $PbZr_3(\mu_4\text{-}O)(\mu\text{-}OAc)_2(O^iPr)_{10}$ for the isopropoxide derivatives.[10a] Studies on alkoxide routes and isolation of $Pb_2Ti_2(\mu_4\text{-}O)(O^iPr)_{10}$, $Pb_4Zr_2(O^iPr)_{16}$, $Pb_3M(\mu_4\text{-}O)(O^iPr)_8$ (M = Ti, Zr) and $PbZr(O^tBu)_6$ have confirmed the influence of the metal and of the OR ligand on the stoichiometry of the Pb–Ti or Pb–Zr species.[11] They have also confirmed the difficulty to accede to Pb–Zr species of 1 : 1 stoichiometry. Studies devoted to the influence of the carboxylate ligands remain scarce and limited to the Pb–Ti system.[10b]

We wish to report herein the study of the molecular constitutions of solutions of lead 2-ethylhexanoate and titanium or zirconium isopropoxides. The first Pb–Ti and Pb–Zr mixed-metal carboxylatoalkoxides whose formulae correspond to simple adducts were isolated and structurally characterized as $Pb_4Zr_4(\mu\text{-}O_2CR')_8(\mu\text{-}OR)_6(\mu_3\text{-}OR)_2(OR)_8(OHR)_2$ **1** and $Pb_2Ti_4(\mu\text{-}O_2CR')_4(\mu\text{-}OR)_6(\mu_3\text{-}OR)_2(OR)_8$ **2** ($R' = CHCH(Et)C_2H_4Me$, $R = {}^iPr$). Their thermal and hydrolytic transformations were investigated. An oxo species of unusual stoichiometry $Pb_2Ti_3(\mu_4\text{-}O)(\mu_3\text{-}O)(\mu\text{-}O_2CC_7H_{15})_2(\mu\text{-}O^iPr)_6(O^iPr)_4$ **3**, was isolated. The various compounds were characterized by elemental analysis, FT-IR, multinuclear NMR (^1H and ^{207}Pb) and for the powders derived from hydrolysis by TGA and XRD.

Results and discussion

Reactions between lead 2-ethylhexanoate and zirconium or titanium isopropoxides at rt

The highly viscous, long chain lead carboxylate, $Pb(O_2CC_7H_{15})_2$ reacts almost immediately at rt in toluene with zirconium or titanium isopropoxides. However, differences in reactivity were observed. Whereas $Zr_2(O^iPr)_8(HO^iPr)_2$ reacts with $[Pb(O_2CC_7H_{15})_2]_m$ giving a species of 1 : 1 stoichiometry, shown

[a]*Université C. Bernard Lyon1, IRC, 2 Avenue A. Einstein, 69 626, Villeurbanne Cedex, France*
[b]*LCC, 205 route de Narbonne, 31077, Toulouse, France. E-mail: Hubert@univ-lyon1.fr*

to be $Pb_4Zr_4(O_2CC_7H_{15})_8(O^iPr)_{16}(HO^iPr)_2$ **1** (eqn (1)), a species of 1 : 2 stoichiometry $Pb_2Ti_4(O_2CC_7H_{15})_4(O^iPr)_{16}$ **2** was obtained with $Ti(O^iPr)_4$ (eqn (2); $R' = C_7H_{15}$).[12] No formation of ester was detected. **1** was isolated in 61% yield by crystallisation in isopropanol. **2** was obtained with either one or two equivalents of $Ti(O^iPr)_4$ reacting with the lead carboxylate although the yield was improved, up to 76%, in the later case.

$$4\,Pb(O_2CR')_2 + 2\,Zr_2(O^iPr)_8(HO^iPr)_2 \rightarrow Pb_4Zr_4(O_2CR')_8(O^iPr)_{16}(HO^iPr)_2 + 2\,Pr^iOH \quad (1)$$

$$2\,Pb(O_2CR')_2 + 4\,Ti(O^iPr)_4 \rightarrow Pb_2Ti_4(O_2CR')_4(O^iPr)_{16} \quad (2)$$

Their spectroscopic data are collected in Table 1. The FT-IR spectra of **1** show absorption bands at 1562, 1422 and 1410 cm^{-1} attributed to the ν_{as} and ν_s stretching vibrations of the CO_2 moiety, respectively. The $\nu_{as}CO_2$ stretching vibrations are shifted to higher frequencies with respect to those of lead 2-ethylhexanoate (1519 cm^{-1}). Similar features are observed for **2**. The differences $\Delta\nu_{as}CO_2 - \nu_sCO_2$, in the range 125–155 cm^{-1}, suggest that the 2-ethylhexanoate ligands are bridging or bridging-chelating for both compounds.[13] The νMOR absorptions are observed between 600 and 400 cm^{-1}. An additional feature for the spectra of **1** is the absorption band at 3390 cm^{-1} suggesting the presence of alcohol in the metal coordination sphere.

The proton NMR spectra of **1** and **2** in $CDCl_3$ confirm the presence of both isopropoxide and carboxylate ligands as well as their relative stoichiometry. The carboxylate resonances are quite broad and mostly uninformative. For **1**, the methine groups of the isopropoxides appear at rt as three well resolved septets at 5.15, 4.59, 4.28 ppm and a broad peak at 4.05 ppm, respectively, with a 4 : 4 : 8 : 2 integration ratio. These spectra are independent of the dilution accounting thus for a single molecular species. No additional resonances are observed at low temperature but the broad peak resolved into a septet, suggesting that it could correspond to isopropanol. ^{207}Pb NMR has also been used since it can provide insights into lead coordination chemistry.[14,15] The spectrum of **1** in toluene shows two main peaks, a broad one centered at 2735 ppm ($\Delta\nu_{1/2}$ = 1268 Hz) and a sharper one at 2653 ppm ($\Delta\nu_{1/2}$ = 397 Hz) in a 1 : 1 ratio. These chemical shifts suggest quite high coordination numbers for the lead centers. ^1H NMR spectra of **2** display peaks with an OR/O_2CR' ratio of four. They resemble to those of **1** and account for at least three types of magnetically non-equivalent isopropoxide ligands with CH signals at 5.42, 4.86 and 4.45 ppm, respectively, in a 4 : 8 : 4 ratio.

Molecular structures of $Pb_4Zr_4(\mu\text{-}O_2CC_7H_{15})_8(\mu_3\text{-}O^iPr)_2(\mu\text{-}O^iPr)_6(O^iPr)_8(^iPrOH)_2$ (1) and of $Pb_2Ti_4(\mu\text{-}O_2CC_7H_{15})_4(\mu_3\text{-}O^iPr)_2(\mu\text{-}O^iPr)_6(O^iPr)_8$ (2). The identity of **1** and **2** as mixed-metal species was established by single-crystal X-ray diffraction. Compound **1** corresponds to $Pb_4Zr_4(\mu\text{-}O_2CR')_8(\mu_3\text{-}OR)_2(\mu\text{-}OR)_6(OR)_8(ROH)_2$ (Fig. 1) and compound **2** to $Pb_2Ti_4(\mu\text{-}O_2CR')_4(\mu_3\text{-}OR)_2(\mu\text{-}OR)_6(OR)_8$ ($R' = C_7H_{15}$, $R = {}^iPr$) (Fig. 2). Selected bond lengths and angles are collected in Tables 2 and 3, respectively.

The basic heterometallic building block (BB) of **1** is a triangular $PbZr_2(OR)_4(\mu\text{-}OR)_3(\mu_3\text{-}OR)(\mu\text{-}O_2CR')$ unit. Two of them are assembled *via* a $Pb_2(O_2CR')_4(OHR)_2$ moiety (Pb–Pb distances of 4.22 Å av.) into a centrosymmetric Pb_4Zr_4 array. All zirconium centers are six-coordinate. The lead atoms belonging to the BB, Pb3, are six-coordinate whereas those who ensure the junctions between the BB *via* a Pb_2O_2 ring, Pb4, are seven coordinate as often observed for lead in a carboxylate ligands environment. All lead centers have a highly distorted stereochemistry. The surrounding of Pb3 corresponds to a trigonal prism whereas that of Pb4 corresponds to a pentagonal bipyramid with O43 and O47 in the axial positions. Distortions are due to the various intracyclic angles [O32–Pb3–O31 of 109.3(2) and 68.2(3)° for $O46^i$–Pb4–O46 for instance] as well as to the small bite angles [48.0(3)–53.0(3)°] of the bridging-chelating carboxylates. The lone pairs on lead appear stereochemically inactive with no obvious vacancy in the first coordination sphere. **1** can thus be considered as holodirected.[16] Although the hydrogen' could not be located, analysis of the M–OR bond lengths on Zr and Pb centers suggest that isopropanol is linked to Pb4 with a bond distance of 2.78(1) Å. Large variations are observed for the Pb–O bond distances [2.343(8)–2.909(7) Å], the longest one corresponding to the Pb–μ_3-OR linkages. Zr–O bond distances spread over the range 1.920(7)–2.230(7) Å. The Zr···Zr distance with a value of 3.527(1) Å is slightly longer than for $Zr_2(O^iPr)_8(^iPrOH)_2$.[17] The Zr–O–C angles of the terminal isopropoxides are large [163.3(1)–171.4(9)°] as common for zirconium alkoxides.[18] A short contact [Pb4···C45 of 2.81(1) Å] is observed with one of the C of the carboxylate ring.

Table 1 ^1H NMR (δ, ppm) and FT-IR data of the Pb–M (M = Ti, Zr) isopropoxide species

		^1H NMR ($CDCl_3$)			IR (cm^{-1})	IR
Compound	T/°C	CH(carb)	OCH(^{i}Pr)	CH_3 (^{i}Pr)	ν_sCO_2, $\nu_{as}CO_2$	νMOR
1	25	2.06 (m, 16 H)	5.15 (sept, J = 6 Hz), 4.59 (sept, J = 6 Hz), 4.28 (sept, J = 6 Hz), 4.05 (br) (4 : 4 : 8 : 2, 18H)	1.18–1.20 (d, 108 H, J = 6 Hz)	1562s, 1533sh, 1410s	644sh, 559s, 462s
	−20	2.06 (m, 16 H)	5.03, 4.54, 4.26, 4.03 (sept, J = 6 Hz) (4 : 4 : 8 : 2, 18H)	1.18–1.20 (d, 108 H, J = 6 Hz)		
2	25	2.05 (m, 8H)	5.42, 4.86, 4.45 (sept, J = 6 Hz) (4 : 8 : 4, 16H)	1.3–1.35 (d, 96 H, J = 6 Hz)	1562s, 1535sh, 1415s	594s, 545m, 520m, 476m
	−58	2.07 (m, 8H)	5.72 (sept, J = 6 Hz), 4.85 (sept, J = 6 Hz), 4.68 (sept, J = 6 Hz) (4 : 8 : 4, 16H)	1.3–1.42 (d, 96H, J = 6 Hz)		
3	25	2.1 m (2H)	5.38 (sept, J = 6 Hz), 5.05 (sept, J = 6 Hz), 4.86 (sept, J = 6 Hz), 4.75 (sept, J = 6 Hz) (2 : 2 : 4 : 2, 10 H)	1.25–1.21 (d, 60 H, J = 6 Hz)	1582vs, 1560sh, 1535sh, 1421s	603vs, 549s, 500sh, 471m

For **1**: νOH 3390 cm^{-1}.

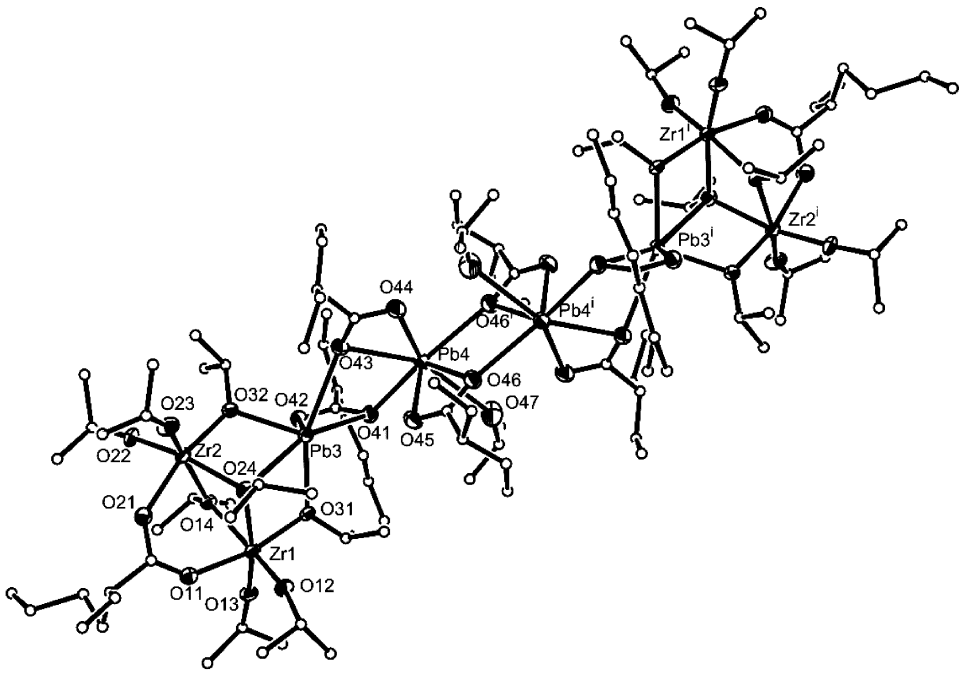

Fig. 1 ORTEP view of **1** with atom labelling for O, Zr and Pb atoms (ellipsoids at 30% probability). C atoms are represented as sphere of arbitrary radius. H atoms as well as the disordered C atoms are omitted for clarity. Symmetry code i: $[1 - x, 1 - y, 1 - z]$.

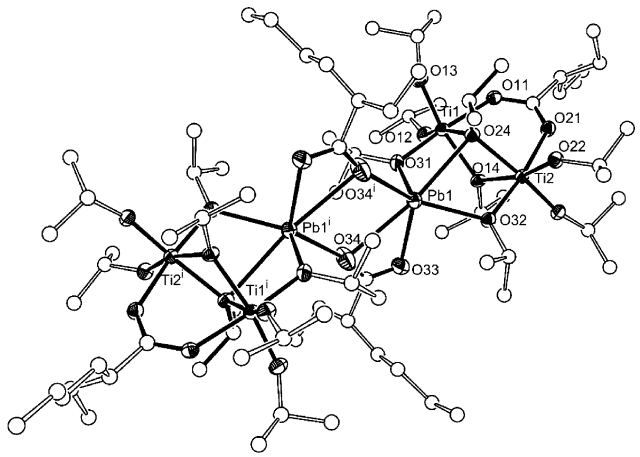

Fig. 2 ORTEP view of **2** with atom labelling for O, Ti and Pb atoms (ellipsoids at 30% probability). C atoms are represented as sphere of arbitrary radius. H atoms as well as the disordered C atoms are omitted for clarity. Symmetry code i: $[x, -y + 1/2, z]$.

The structure of **2** is also centrosymmetric and based on triangular $Ti_2Pb(O_2CR')(OR)_8$ units similar to those observed for **1**. The main difference with **1** lies in the connection between the BB. For **2**, the BB are linked by their lead atoms *via* bridging-chelating μ,η^2-carboxylate ligands and its overall stoichiometry is thus that of the BB. This results in a slightly asymmetrical bridge [2.803(6) and 2.909(7) Å] and in six-coordinate lead centers due to Pb–μ_3-OR bonds. The Ti–O bond distances range from 1.785(5) to 2.137(5) Å and vary in the order Ti–OR(t) < Ti-μ-OR < Ti–O_2CR' as expected. The M · · · M distance [3.308(1) Å] is shorter than in the case of zirconium. The Pb–O bond lengths vary from 2.331(5) to 2.909(7) Å, the longest ones corresponding to the carboxylate and μ_3-OR bridges. The Ti–O–C angles of the terminal OR are smaller than for **1** as usually observed.[10]

Triangular BB are quite common for heterometallics based on a MM'_2 stoichiometry although they are often capped by two triply bridged ligands.[19] A large number of heterometallic species involving zirconium are based on the $[Zr_2(OR)_9]^-$ moiety.[18,20] An alternative description of the structures of **1** and **2** is based on the $[M_2(\mu\text{-}OR)_3(\mu_3\text{-}OR)(\mu\text{-}O_2CR')(OR)_4]^-$ moiety trapping $Pb_2(O_2CR')_3(ROH)^+$ or $Pb(O_2CR')^+$ units, respectively. In contrast with the Pb–M heterometallic species based on acetates,[10] the 2-ethylhexanoate ligands display two types of coordination modes, bridging and bridging-chelating. The related Pb–O bond distances are quite long as compared to usual Pb–O(carboxylate) ones. No solid state data are available for lead 2-ethylhexanoate but the lead carboxylates are reported as oligomers due to the assembling behavior of the O_2CR' ligands and as illustrated by lead succinate $[Pb(O_4C_4H_4)]_\infty$ for instance.[21] Metal alkoxides depolymerize metal acetates giving heterometallic acetatooxoalkoxides.[10,22] Depolymerization of lead 2-ethylhexanoate is also achieved here, the difference in the frameworks of **1** and **2** reflecting the lower reactivity of $Zr_2(O^iPr)_8(^iPrOH)_2$ as compared to $Ti(O^iPr)_4$ for formation of MM' species.[6,18,23] Reactions between anhydrous lead acetate, insoluble, and group 4 alkoxides afforded only oxo heterometallic species even for reactions achieved at rt.[10] The acetate ligands usually bridge the two types of metals but the presence of oxo ligands implies more structural reorganization than here, especially in the case of zirconium isopropoxide.[10a] The solubility of lead 2-ethylhexanoate in non-polar media allows formation of a mixed-metal Pb–Zr species without complete breakdown of the chelating-bridging Pb carboxylate array. Another observation is that for heterometallics involving lead acetate, lead displays stereochemically active lone pairs and lower coordination numbers. It is noteworthy that adducts **1** and **2** were

Table 2 Selected bond lengths (Å) and angles (°) for $Pb_4Zr_4(\mu\text{-}O_2CR')_8(\mu\text{-}OR)_6(\mu_3\text{-}OR)_2(OR)_8(OHR)_2$ **1**

O1–1Zr1	2.190(8)	O14–Zr2	2.171(7)
O12–Zr1	1.934(8)	O21–Zr2	2.206(8)
O13–Zr1	1.920(7)	O22–Zr2	1.946(8)
O24–Zr1	2.239(7)	O23–Zr2	1.938(8)
O31–Zr1	2.082(7)	O24–Zr2	2.230(7)
O14–Zr1	2.189(7)	O32–Zr2	2.079(7)
Zr1–Zr2	3.527(1)		
Pb3–Zr1	3.782(1)		
Pb3–Zr2	3.771(1)	O41–Pb4	2.615(8)
Pb3–Pb4	4.191(1)	O41–Pb4	2.597(8)
Pb4–Pb4[a]	4.257	O43–Pb4	2.604(8)
O31–Pb3	2.399(6)	O44–Pb4	2.463(8)
O42–Pb3	2.343(8)	O32–Pb3	2.386(7)
O41–Pb3	2.882(8)	O45–Pb4	2.403(8)
O24–Pb3	2.909(7)	O46–Pb4	2.460(8)
O43–Pb3	2.847(7)	O46–Pb4#	2.679(8)
		O47–Pb4	2.78(1)
Zr2–O14–Zr1	108.0(3)		
Zr2–O24–Zr1	104.2(3)		
Zr1–O31–Pb3	114.9(3)		
Zr2–O32–Pb3	115.1(3)		
O42–Pb3–O32	82.2(3)	O42–Pb3–O24	127.7(2)
O42–Pb3–O31	92.6(3)	O32–Pb3–O24	65.1(2)
O32–Pb3–O31	109.3(2)	O31–Pb3–O24	64.3(2)
O42–Pb3–O41	48.0(3)	O41–Pb3–O24	158.6(2)
O32–Pb3–O41	126.1(3)	O43–Pb3–O31	156.1(3)
O31–Pb3–O41	94.3(2)		
O13–Zr1–O12	99.0(3)	O31–Zr1–O11	167.4(3)
O13–Zr1–O31	98.6(3)	O14–Zr1–O11	83.4(3)
O12–Zr1–O31	97.5(3)	O13–Zr1–O24	165.5(3)
O13–Zr1–O14	94.9(3)	O12–Zr1–O24	95.1(3)
O12–Zr1–O14	163.9(3)	O31–Zr1–O24	82.8(3)
O31–Zr1–O14	88.4(3)	O14–Zr1–O24	70.7(3)
O13–Zr1–O11	91.7(3)	O11–Zr1–O24	85.5(3)
O12–Zr1–O11	88.0(3)		
O23–Zr2–O22	100.8(4)	O22–Zr2–O21	89.9(3)
O23–Zr2–O32	99.9(3)	O32–Zr2–O21	167.2(3)
O22–Zr2–O32	97.8(3)	O14–Zr2–O21	83.7(3)
O23–Zr2–O14	162.0(3)	O23–Zr2–O24	92.1(3)
O22–Zr2–O14	95.4(3)	O22–Zr2–O24	166.4(3)
O32–Zr2–O14	85.5(3)	O32–Zr2–O24	83.9(3)
O23–Zr2–O21	88.5(3)	O14–Zr2–O24	71.2(3)
		O21–Zr2–O24	86.2(3)

Symmetry transformation used to generate equivalent atoms:[a] $-x + 1, -y + 1, -z + 1$.

Table 3 Selected bond lengths (Å) and angles (°) for $Pb_2Ti_4(\mu\text{-}O_2CR')_4(\mu\text{-}OR)_8(\mu_3\text{-}OR)_2(OR)_8$ **2** ($R' = CHCH(Et)C_2H_4Me$)

Pb1–O31	2.331(5)		
Pb1–O33	2.366(5)		
Pb1–O32	2.395(5)		
Pb1–O34	2.803(6)		
Pb1–O34[a]	2.909(7)		
Pb1–O24	2.849(6)		
Ti1–O13	1.795(5)		
Ti1–O12	1.804(5)	Ti2–O23	1.785(5)
Ti1–O31	1.973(5)	Ti2–O22	1.805(4)
Ti1–O14	2.021(5)	Ti2–O32	1.963(5)
Ti1–O11	2.081(5)	Ti2–O14	2.071(4)
Ti1–O24	2.137(5)	Ti2–O24	2.075(5)
		Ti2–O21	2.096(5)
Ti1–Ti2	3.308(2)		
Pb1–Ti2	3.658(2)		
Pb1–Ti2	3.630(2)		
Pb1–Pb1[a]	4.617(2)		
O31–Pb1–O33	92.1(2)	O32–Pb1–O34	125.4(2)
O31–Pb1–O32	106.5(2)	O31–Pb1–O34	109.9(2)
O33–Pb1–O32	85.2(2)	O33–Pb1–O34	121.2(2)
O31–Pb1–O34	104.2(2)	O32–Pb1–O34	133.1(2)
		O33–Pb1–O34	49.5(2)
O13–Ti1–O12	98.8(2)	O11–Ti1–O24	87.9(2)
O13–Ti1–O31	95.1(2)		
O12–Ti1–O31	95.7(2)	O23–Ti2–O22	97.2(2)
O13–Ti1–O14	163.8(2)	O23–Ti2–O32	96.1(2)
O12–Ti1–O14	96.4(2)	O22–Ti2–O32	96.9(2)
O31–Ti1–O14	89.2(2)	O23–Ti2–O14	95.3(2)
O13–Ti1–O11	87.5(2)	O22–Ti2–O14	166.2(2)
O12–Ti1–O11	90.5(2)	O32–Ti2–O14	87.3(2)
O31–Ti1–O11	172.7(2)	O23–Ti2–O24	166.8(2)
O14–Ti1–O11	86.5(2)	O22–Ti2–O24	95.4(2)
O13–Ti1–O24	93.3(2)	O32–Ti2–O24	86.0(2)
O12–Ti1–O24	167.8(2)	O14–Ti2–O24	71.7(2)
O31–Ti1–O24	85.3(2)	O23–Ti2–O21	88.4(2)
O14–Ti1–O24	71.5(2)	O22–Ti2–O21	90.1(2)
O32–Ti2–O21	171.1(2)		
O14–Ti2–O21	84.7(2)		
Ti2–O32–Pb1	113.8(2)		
Ti1–O14–Ti2	107.8(2)		
Ti2–O24–Ti1	103.5(2)		
Ti1–O31–Pb1	114.8(2)		

Symmetry code to generate equivalent atoms:[a] $x, -y + 1/2, z$.

isolated in high yields despite the presence of water (~0.5%) in commercial lead 2-ethylhexanoate.

Single-crystal data of 2-ethylhexanoate derivatives, often considered as metallic soaps, remain very scarce since the long chain carboxylates favor disorder and the obtaining crystals of poor quality.[24] These limitations are valid here, especially for compound **1**, but the solid state structures are supported by the ^1H and ^{207}Pb NMR spectra. The latter displaying two signals with a 1 : 1 integration ratio for **1** suggest that its solid state structure is retained in solution. ^{207}Pb NMR data on seven-coordinated lead species are scarce. A chemical shift of 1667 ppm has been reported for heptacoordinate lead in $Pb_6(O_2C^iPr)_{12}$.[15] The data obtained for **1** indicate only a difference of 100 ppm for the six- and seven fold-coordinate lead centers. The ^1H NMR data of **1** and **2** suggest that the chemical shifts of the μ_3-OR and μ-$OR_{(MM)}$ ligands are similar or that the quite long Pb–μ_3-OR bonds are broken in solution, reducing the coordination number of the corresponding lead atoms to five in solution. Compounds **1**, **2** and **3** (see below) are, to the best of our knowledge, the first examples of mixed-metal species with 2-ethylhexanoate ligands.

Reactivity studies of the Pb–Zr and Pb–Ti species

Hydrolysis of 1 and of 2. Hydrolysis of **1** in 0.05 M THF solutions at rt with hydrolysis ratios $h = 0.2$–1 gives clear solutions (h = mol H_2O/mol precursor). Those remain homogeneous for over two months although a slight increase in viscosity occurs. Hydrolysis of **1** and **2** in the parent alcohol at rt (0.05 M) affords solutions for $h = 0.2$–0.4, but precipitates for $h = 1$ or 2. More concentrated media favor the formation of gels.

The obtaining of homogeneous solutions by hydrolysis allows some ^1H NMR monitoring in $CDCl_3$. Hydrolysis was immediate for **1** and **2**. The resulting spectra were characterized in the CH region of the O^iPr ligands by decrease of the initial peaks, apparition of new sets of resonances as well as apparition (for **2**) or increase (for **1**) of the peak of isopropanol. The latter shifts to higher

frequencies with the extent of hydrolysis suggesting exchange between coordinated and free alcohol molecules. The first hydrolytic steps are likely to be intramolecular as observed for $BaZr_4(OR)_{18}$.[25] and to proceed at the electrophilic metals, zirconium or titanium and on their bridging alkoxide ligands.[26] This should affect the μ_3-OR and transform the $[PbM_2(\mu_3\text{-}OR)(\mu\text{-}OR)(\mu\text{-}OR)_2(\mu\text{-}O_2CR')(OR)_4]^+$ building blocks units into $[PbM_2(\mu_3\text{-}O)(\mu\text{-}OR)_2(\mu\text{-}O_2CR')(OR)_4]^+$ ones. This is confirmed by the development of species having two types of OR ligands in a 8 : 4 integration ratio in both cases, namely 4.90, 4.70 and 5.38, 5.68 ppm for **1a** (M = Zr) and **2a** (M = Ti), respectively. This transformation would leaves the transition metals M five-coordinate, quite unlikely for zirconium with O^iPr ligands. However, the chemical shift of isopropanol suggests coordination to the transition metals of some of the alcohol molecules eliminated by hydrolysis. Eqn (3) and (4) summarizes these first hydrolytic steps whereas Scheme 1 represents structures of **1a** and **2a** based on six-coordinate transition metals in agreement with the ^1H NMR data. All attempts to isolate **1a** or **2a** in crystalline form were unsuccessful.

$$\mathbf{1} + 2\,H_2O \rightarrow Pb_4Zr_4(\mu_3\text{-}O)_2(\mu\text{-}O_2CR')_8(OR)_{12}(ROH)_x\ (\mathbf{1a}) + (6 - x)\,ROH \quad (3)$$

$$\mathbf{2} + 2\,H_2O \rightarrow Pb_2Ti_4(\mu_3\text{-}O)_2(\mu\text{-}O_2CR')_4(OR)_{12}(ROH)_x\ (\mathbf{2a}) + (4 - x)\,ROH \quad (4)$$

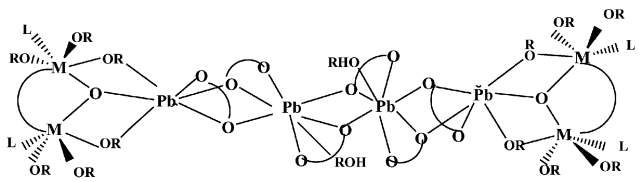

1a

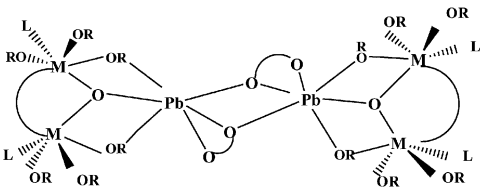

2a

Scheme 1

1a and **2a** were also detected, in small amounts (~5%) in the reaction medium. Their presence, while no ester was detected, is most likely due to hydrolysis by the traces of water in commercial lead 2-ethylhexanoate.[12]

Hydrolysis at higher hydrolysis ratio is likely to affect $\mu\text{-}OR_{(PbM)}$ and terminal OR ligands, the condensation becoming intermolecular and leading to more drastic structural modifications. For instance, hydrolysis at $h = 8$ of **1** gives spectra displaying the peak of free isopropanol, two main septuplets at 4.68 and 4.28 ppm and numerous smaller broad peaks (up to eight of similar area spreading over the range 6.1–4.20 ppm at −20 °C) belonging to a same species as shown by dilution experiments. These observations account for formation of oligomers due to extensive condensation with a large number of magnetically non-equivalent OR ligands. The last hydrolytic steps involve elimination of some 2-ethylhexanoic acid (FT-IR evidence). Elimination of acid is also confirmed by the obtaining of a powder analyzing as $PbZrO(O_2CR')(ROH)$ by hydrolysis at rt of **1** by an excess of water.

The $PbZrO_3$ (PZ) perovskite is one of least stable and thus difficult to obtain lead based perovskite.[6] Hydrolysis of **1**, whose stoichiometry matches that of PZ, was thus also achieved with an excess of water ($h = 70$) in isopropanol. FT-IR data of the amorphous powder obtained show residual carboxylate ligands ($\nu_{as}CO_2$ 1540, ν_sCO_2 1409 cm^{-1}) as expected for differential hydrolysis.[7] Its TGA and DTA patterns display several strong exothermic peaks for combustion of the residual organics which occurs in quite mild conditions (250–450 °C). A total weight loss of 37% suggests that the powder has a composition $PbZrO(O_2CR')(ROH)$ (theoretical loss 37.8%). Annealing of the powder under air afforded a crystalline material. Crystallization starts around 450 °C and was analyzed in terms of formation of pyrochlore.[6] Crystallization of the PZ perovskite starts around 550 °C and a pure perovskite phase is obtained at 600 °C. Thus the use of a single-source precursor (SSP) allows to avoid segregation and gives access to crystalline PZ at ~100 °C lower than by using mixtures in which no homogeneity at a molecular level is achieved.[6] Hydrolysis of **2** affords $PbTi_3O_7$ as well as red lead oxide as observed for the previously reported $PbTi_2$ species.[10a]

Thermal reactions between with Ti or Zr isopropoxides and Pb 2-ethylhexanoate. Molecular structure of $Pb_2Ti_3O_2(O_2CR')_2(OR)_{10}$ 3. The formulae of **1** and **2** correspond to Lewis acid base adducts between the reagents. Heating is often used in order to stabilize stock solutions for applications.[6] Its effect on the molecular constitutions of solutions of lead 2-ethylhexanoate and $Zr_2(O^iPr)_8(^iPrOH)_2$ or $Ti(O^iPr)_4$, in 1 : 1 and 1 : 2 stoichiometry, respectively, in toluene was thus investigated. No formation of ester was observed for short heating times (15 min, 80 °C) and spectroscopic data showed only a slight increase of the amount of **1a** and **2a** due to hydrolysis.[12] Analysis of the volatiles (by FT-IR and GPC) after further heating, 10 h at 120 °C or 6 h at 120 °C, actually the conditions for complete condensation in toluene and getting thermodynamically stable compounds, **1b** and **2b**, shows elimination of isopropanol and formation of isopropyl-2-ethyl hexanoate (νCO_2 1733 cm^{-1}). Extensive heating generates thus metallic oxo species as also illustrated by the strong absorption bands in the IR spectra in the 800–600 cm^{-1} region. The presence in the volatiles of ester (~55%) but also of isopropanol (~45%), even for compound **2** indicates thus that both hydrolytic and non-hydrolytic processes occur when using commercial Pb 2-ethylhexanoate in the MOD process.[6] Elemental analyses of the pasty solids obtained after heating and elimination of the volatiles account for formation of $[Pb_4Zr_4O_8(O_2CR')_4(O^iPr)_4]_m$ and $[Pb_2Ti_4O_8(O_2CR')_2(O^iPr)_2]_m$ oligomers. ^1H NMR data confirm that half of the carboxylate ligands are eliminated in both Pb–Zr and Pb–Ti systems despite the difference in the initial OR : O_2CR' stoichiometry. Similar NMR patterns were obtained (six broad peaks for instance for **1b** ranging from 4.87 to 4.22 ppm with a 2 : 3 : 2 : 3 : 2 integration ratio) suggesting a value of at least three for the degree of association, *m*. Condensation into large oligomers and thus elimination of the organic ligands appears faster by hydrolysis than by heating.

Condensation of the Pb_2Ti_4 species, **2**, is also faster than that of the Pb_4Zr_4 one **1** since no more evolution of **2** was observed after heating for 6 h at 120 °C. After removal of the volatiles of that reaction medium under vacuum (60 °C/10^{-3} mm Hg), compound **3** could be crystallized in ~25% by adding isopropanol to the crude product. Elemental analyses account for a Pb/Ti ratio of 2 : 3. This change in the Pb/Ti stoichiometry is confirmed by isolation of titanium isopropoxide by fractional distillation of the volatiles. The FT-IR spectrum of **3** accounts for an oxo species as illustrated by absorption bands at 837, 784, 704 cm^{-1}. Its ^1H NMR spectra indicate a 10 : 2 ratio for the O^iPr:O_2CR' ligands and four signals in the methine region at 5.38, 5.05, 4.86 and 4.35 ppm in a 2 : 2 : 4 : 2 ratio. The ^{207}Pb NMR data show two sharp peaks of comparable intensities at 3005 and 2682 ppm.

Despite the unusual $M_2M'_3$ stoichiometry, the structure of compound **3**, $Pb_2Ti_3(\mu_4\text{-}O)(\mu_3\text{-}O)(\mu\text{-}O_2CC_7H_{15})_2(\mu\text{-}O^iPr)_6(O^iPr)_4$ appears quite symmetrical (Fig. 3). Selected bond distances and angles are collected in Table 4. **3** can be seen as a $Pb_2Ti_2O_2(\mu\text{-}O_2CR')_2(OR)_6$ species having two types of oxo ligands namely a central μ_4 one O2 and a peripheral one O1 which acts as ligand toward a $Ti(O^iPr)_4$ moiety leading to a five-coordinate Ti. Such coordination of an alkoxide by a peripheral oxo ligand has been observed for $Pb_6Nb_4O_4(OEt)_{24}$.[27] This μ_3-oxo ligand O1 has a quite regular planar trigonal geometry. In contrast, the stereochemistry of the tetragonal oxo ligand is distorted with an increase in the Ti2 ··· Ti2 distance up to 3.608 Å (as compared to **2**), as well as an opening of the Ti2O2Ti2 angle [up to 136.2(4)°] for accommodation of the two bridging carboxylates. The Ti–O bond distances spread over the range 1.791(7) to 2.112(6) Å with the ranking Ti–OR < Ti-μ_3O ≈ Ti-μOR < Ti-μ_4-O < Ti-$\mu O_2CR'$. The Pb–O bond distances are longer [2.161(4)–2.555(6) Å] and vary along Pb-μ_3O < Pb-μ_4O < Pb–OR but they are shorter than for **1** and **2** due to the lower coordination numbers of lead. The Pb–OR–Ti bridges are quite asymmetrical. In contrast with **1** and **2**, the lone pairs of the five-coordinate tetragonal pyramidal lead centers are stereochemically active. Compound **3** can also be seen as the association of two PbO units, $Ti(OR)_4$ and $Ti_2(O_2CR')_2(OR)_6$.

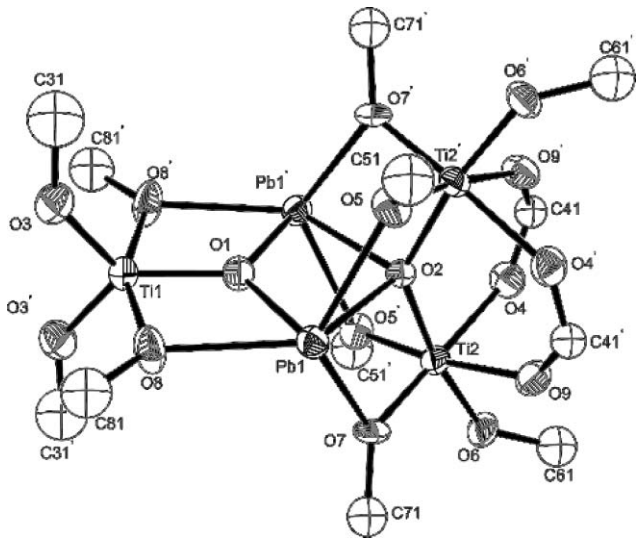

Fig. 3 ORTEP view of **3** with atom labelling for O, Ti and Pb atoms (ellipsoids at 30% probability). C atoms are represented as sphere of arbitrary radius. H atoms as well as the disordered C atoms are omitted for clarity. Symmetry code i: [$-x$, y, $-z + 1/2$].

Table 4 Selected bond lengths (Å) and angles (°) for $Pb_2Ti_3(\mu_4\text{-}O)(\mu_3\text{-}O)(\mu\text{-}O_2CC_7H_{15})_2(\mu\text{-}O^iPr)_6(O^iPr)_4$ **3**

Ti1–O3	1.791(7)	O1–Ti1	1.873(7)
Ti1–O8	1.959(6)	O6–Ti2	1.805(6)
O4–Ti2	2.093(6)	O9–Ti2	2.112(6)
O5–Ti2	1.894(6)	O2–Ti2	1.944(3)
O8–Ti1	1.959(6)	O7–Ti2	1.896(6)
O5–Pb1	2.506(6)	O2–Pb1	2.462(4)
O8–Pb1	2.548(6)	O7–Pb1	2.555(6)
O1–Pb1	2.161(4)		
Ti2–Ti2	3.608(2)		
Ti1–Pb1	3.498(2)		
Ti2–Pb1	3.478(2)		
Ti2–Pb1	3.497(2)		
Ti2–O5–Pb1	103.6(2)	Ti2–O2–Pb1	104.46(9)
Ti1–O8–Pb1	101.0(2)	Ti2–O2–Pb1	103.64(9)
Ti1–O1–Pb1	120.1(2)	Ti2–O2–Pb1	104.46(9)
Pb1–O1–Pb1	119.8(3)	Pb1–O2–Pb1	98.8(2)
Ti2–O2–Ti2	136.2(4)	Ti2–O7–Pb1	102.6(2)
O3–Ti1–O3	105.3(4)	O6–Ti2–O2	169.6(3)
O3–Ti1–O1	127.4(2)	O5–Ti2–O2	87.8(2)
O3–Ti1–O1	127.4(2)	O7–Ti2–O2	88.3(2)
O3–Ti1–O8	97.5(3)	O6–Ti2–O4	86.0(3)
O3–Ti1–O8	97.1(3)	O5–Ti2–O4	172.2(3)
O1–Ti1–O8	77.9(2)	O7–Ti2–O4	89.4(3)
O1–Ti1–O8	77.9(2)	O6–Ti2–O9	85.7(3)
O8–Ti1–O8	155.8(3)	O5–Ti2–O9	89.1(3)
O6–Ti2–O5	98.7(3)	O7–Ti2–O9	172.5(3)
O6–Ti2–O7	99.0(3)	O2–Ti2–O9	86.3(2)
O5–Ti2–O7	95.9(3)	O4–Ti2–O9	85.1(3)
O1–Pb1–O2	70.7(2)		
O1–Pb1–O5	94.1(2)		
O2–Pb1–O5	64.8(1)		
O1–Pb1–O8	60.9(2)		
O2–Pb1–O8	131.5(2)		
O5–Pb1–O8	114.5(2)		
O1–Pb1–O7	93.4(2)		
O2–Pb1–O7	64.5(1)		
O5–Pb1–O7	122.2(2)		
O8–Pb1–O7	118.8(2)		

The formation of **3** results from a drastic reorganization of compound **2** by elimination of $Ti(OR)_4$ as summarized by eqn (5). Spectroscopic data (^1H NMR, FT-IR) of the crude product obtained after heating of **2** before elimination of volatiles gave evidence for traces of titanium isopropoxide. However, the passage from a Pb_2Ti_4 stoichiometry to a Pb_2Ti_3 one is favored by the treatment under vacuum and the volatility of $Ti(O^iPr)_4$. The 2-ethylhexanoate ligands linked to lead appear more labile than those on titanium. This lability and the tendency to form oxo species was also observed by long heating of $Pb(O_2CR')_2$ during its synthesis from lead oxide. ^1H and ^{207}Pb NMR spectra account for the retention of the solid state structure of **3** by dissolution in non-polar media.

$$Pb_2Ti_4(O_2CR')_4(OR)_{16} \xrightarrow{\Delta} Pb_2Ti_4O_2(O_2CR')_2(OR)_{10} + 2RCO_2R' \quad (5)$$

$$Pb_2Ti_4(O_2CR')_2(OR)_{10} \xrightarrow{\Delta(\text{vacuum})} Pb_2Ti_3O_2(O_2CR')_2(OR)_{10} + Ti(OR)_4 \quad (6)$$

Experimental

All manipulations were performed under argon using Schlenk tubes and vacuum line techniques with solvents purified by standard methods. Lead 2-ethylhexanoate (Strem) was used as received. $Ti(O^iPr)_4$ (Aldrich) was purified by distillation and $Zr_2(O^iPr)_8(^iPrOH)_2$ was synthesized as reported.[17] Hydrolyses were achieved at rt in THF or in the parent alcohol. Water was added *via* the same solvent. The resulting powders were separated by filtration. ^1H and ^{207}Pb NMR spectra (52.3 MHz) were recorded on a Bruker AC-250 spectrometer. Lead chemical shifts are given with respect to $Pb(NO_3)_2$ as external reference. IR spectra were run on a Paragon 500 FT-IR spectrometer, they were obtained as Nujol mulls for the air-sensitive species, as KBr pellets for the hydrolyzed ones. Analytical data were obtained from the Centre de Microanalyses du CNRS. TGA/DTA data were collected on a Setaram 92 system in air with a thermal ramp of 5 °C min^{-1}. XRD were obtained with a Siemens D 500 diffractometer (Cu-Kα radiation). Spectroscopic data (NMR, FT-IR) are collected in Table 1.

Synthesis of $Pb_4Zr_4(O_2CC_7H_{15})_8(O^iPr)_{16}(HO^iPr)_2$ (1)

$[Zr(O^iPr)_4(HO^iPr)]_2$ (1.67 g, 4.31 mmol) in toluene was added to $Pb(O_2CC_7H_{15})_2$ (2.13 g, 4.31 mmol) in 10 ml of toluene. The medium was stirred at rt for 10 h. Elimination of the volatiles *in vacuo* gave an oil. Addition of isopropanol gave **1** as colorless crystals at −10 °C [2.25 g, 61%/$Pb(O_2CC_7H_{15})_2$]. **1** was poorly soluble in isopropanol, more soluble in toluene or hexane. Anal. Calc. For $C_{118}H_{248}O_{34}Pb_4Zr_4$: (3260.52) C, 41.63; H, 7.34, Pb, 24.34; Zr, 10.72. Found: C, 41.85; H, 7.45; Pb, 25.03; Zr, 11.20%. $^{207}Pb\{^1H\}$ NMR (toluene, ppm): 2735 (broad), 2653 (1 : 1).

Synthesis of $Pb_2Ti_4(O_2CC_7H_{15})_4(O^iPr)_{16}$ 2

The same procedure applied to $Ti(O^iPr)_4$ (2.87 ml, 9.66 mmol), $Pb(O_2CC_7H_{15})_2$ (2.38 g, 4.83 mmol) in 20 ml of toluene and addition of ^{i}PrOH–hexane (1 2 in volume) gave **2** (3.92 g, 76%/$Pb(O_2CC_7H_{15})_2$). **2** was poorly soluble in hexane, more soluble in toluene and isopropanol. Anal. Calc. For $C_{80}H_{174}O_{24}Pb_2Ti_4$ (2120.12): C, 45.19; H, 8.25; Pb; 19.46; Ti, 9.01. Found: C, 45.54; H, 8.32; Pb, 20.82; Ti, 9.45%. $^{207}Pb\{^1H\}$ NMR (toluene, ppm): 2944

Synthesis of $Pb_2Ti_3O_2(O_2CC_7H_{15})_2(O^iPr)_{10}$ 3

$Ti(O^iPr)_4$ (1.82 ml, 6.12 mmol) was added to $Pb(O_2CC_7H_{15})_2$ (1.51 g, 3.06 mmol). After heating at 120 °C for 6 h, the yellow oil was distilled (60 °C/10^{-3} mm Hg) to remove the by-products. Addition of 6 ml of isopropanol to the residue gave a solid **3** at −20 °C (0.75 g, 0.51 mmol, 25%/Ti, 33%/Pb). **3** was soluble in isopropanol, THF and hydrocarbons. Anal. Calc. for $C_{46}H_{100}O_{16}Ti_3Pb_2$ (1463.30): C, 37.65; H, 6.87; Pb, 28.24; Ti, 9.79, Found C 38.05, H, 6.93, Pb 28.72, Ti, 9.83%. $^{207}Pb\{^1H\}$ NMR (toluene, ppm): 3005 (65 Hz), 2682 (85 Hz) (1 : 1).

Crystal structure determination of 1, 2 and 3

Single crystals of **1** and **3** were obtained from isopropanol, those of **2** were obtained in isopropanol–hexane. They were mounted under inert perfluoropolyether on a glass fiber and cooled in the cryostream of the diffractometer. Data were collected at 180(2) K using the monochromatic Mo-Kα radiation. The structures were solved by direct methods (SIR97)[28] and refined by least-squares on F^2 using SHELXL-97.[29] All H atoms attached to carbon were introduced in idealized positions [d(CH) = 0.96 Å] and treated as riding models. In **3**, some of the carbon atoms of the alkoxide ligands presented large ellipsoids and disordered models to better fit the electron density were applied using the available tools (PART and DFIX) in SHELXL-97. In **2**, owing to the low number of data, the C atoms were refined isotropically. As in **3**, some of the alkyl chains were disordered and treated accordingly. In **1**, the anisotropic thermal parameters for C atoms are very large but no disordered models could be defined. The drawings were done with ORTEP-32.[30] Crystal data and refinement parameters are shown in Table 5.

Table 5 Summary of crystallographic data for **1**, **2** and **3** at 180 K

	1	**2**	**3**
Empirical formula	$C_{108}H_{224}O_{34}Pb_4Zr_4$	$C_{80}H_{168}O_{24}Pb_2Ti_4$	$C_{46}H_{96}O_{16}Pb_2Ti_3$
M_r	3260.52	2120.03	1463.3
Space group	$P\bar{1}$	$P\bar{1}$	$C2/c$
Crystal system	Triclinic	Triclinic	Monoclinic
a/Å	11.377(1)	11.3722(6)	21.663(2)
b/Å	13.118(1)	12.4435(6)	14.231(1)
c/Å	26.190(3)	19.303(1)	22.737(2)
α/°	85.559(8)	91.624(4)	90
β/°	83.667(7)	96.393(4)	116.342(8)
γ/°	76.410(8)	109.728(5)	90
V/Å^3	3771.0(6)	2549.0(2)	6281.7(9)
Z	1	1	4
Diffractometer	Oxford X-CALIBUR CCD	Stoe IPDS	Oxford X-CALIBUR CCD
μ(Mo-Kα)/mm^{-1}	4.772	3.650	5.762.
No. of unique reflections (R_{int})	10765(0.0674)	6680 (0.0848)	4824 (0.0485)
Absorption correction	Analytical	Semi-empirical from equivalents	Semi-empirical from equivalents
Data/restraints/parameters	10765/772/704	6680/480/544	4824/15/219
Goodness-of-fit on F^2	1.069	1.059	1.081
R_1, wR_2 [$I > 2\sigma(I)$][a]	0.0438, 0.1165	0.0554, 0.1484	0.0432, 0.1156
R_1, wR_2 (all data)	0.0568, 0.1225	0.0637, 0.1586	0.0553, 0.1216

[a] $R_1 = \sum\|F_o| - |F_c\|/\sum|F_o|$, $wR_2 = [\sum[w(F_o^2 - F_c^2)^2]/\sum[w(F_c^2)^2]]^{1/2}$.

CCDC reference numbers 230776–230778 for **2**, **3** and **1**, respectively.

For crystallographic data in CIF or other electronic format see DOI: 10.1039/b513142c

Conclusion

The molecular constitution of solutions of Ti and Zr alkoxides and lead carboxylates is function of the alkoxide as well as of the carboxylate ligands. The first non-oxo Ti–Pb and Zr–Pb carboxylatoalkoxides have being obtained at rt with 2-ethylhexanoate as carboxylate ligands. heir stoichiometry is 1 : 1 in the case of zirconium but 1 : 2 for titanium, independently of the ratio between the reagents. Compound **1**, $Pb_4Zr_4(\mu\text{-}O_2CR')_8(\mu\text{-}OR)_6(\mu_3\text{-}OR)_2(OR)_8(OHR)_2$, is thus the first Pb–Zr carboxylatoalkoxide of 1 : 1 stoichiometry reported and thus matching the formula of the $PbZrO_3$ (PZ) ceramic, this stoichiometry being not accessible with acetate as ligands. Evaluation of their condensation by hydrolysis and by heating shows that formation of extensive arrays is faster by hydrolysis. The volatility of $Ti(O^iPr)_4$ can promote a change in the stoichiometry of the Pb_2Ti_4 species by heating giving the $Pb_2Ti_3(\mu_4\text{-}O)(\mu_3\text{-}O)(\mu\text{-}O_2CC_7H_{15})_2(\mu\text{-}O^iPr)_6(O^iPr)_4$ oxo species **3**. Compounds **1**, **2** and **3** are, to the best of our knowledge, the first structurally characterized mixed-metals species with 2-ethylhexanoate ligands. The Pb–Zr single source precursor favors access to PZ at low temperature.

Acknowledgements

We are grateful to Protavic for financial support.

References

1 (*a*) N. Setter, *J. Eur. Ceram. Soc.*, 2001, **21**, 1279; (*b*) C. D. Chandler, C. Roger and J. M. Hampden-Smith, *Chem. Rev.*, 1993, **93**, 1205–1241; (*c*) S. T. Swartz and V. E. Wood, *Condens. Matter News*, 1992, **1**, 4–28.
2 C. H. Peng and S. B. Desu, *J. Am. Ceram. Soc.*, 1994, **77**, 1799; T. Katoyama, M. Fujimato, M. Shimizu and T. Shiosaki, *J. Cryst. Growth*, 1991, **115**, 289.
3 C. E. Lakeman and D. Payne, *J. Am. Ceram. Soc.*, 1992, **75**, 309; T. J. Boyle, D. Dimos, R. W. Schwartz, T. M. Alam, M. B. Sinclair and C. D. Buchheit, *J. Mater. Res.*, 1997, **12**, 1022–1030; R. W. Schwartz, J. A. Voigt, B. A. Tutle, D. A. Payne, T. L. Reichert and R. S. Dasalla, *J. Mater. Res.*, 1997, **12**, 444–456; T. Fukui, C. Sakurai and M. Okuyama, *J. Mater. Res.*, 1992, **7**, 791–794.
4 P. Gaucher, J. Hector, J. C. Kurfiss, in *Science and Technology of Electroceramic Thin Films*, ed. O. Auciello and R. Waser, Kluwer, Dordrecht, Netherlands, 1995, p. 147; S. Morlens, L. Ortega, B. Rousseau, S. Phok, J. L. Deschanvres, P. Chaudouet and P. Odier, *Mater. Sci. Eng. B*, 2003, **104**, 185; A. A. Avey and R. H. Hill, *J. Am. Chem. Soc.*, 1996, **118**, 237–238.
5 M. L. Calzada, F. Carmona, R. Sirera and B. Jimenez, *J. Am. Ceram. Soc.*, 1995, **78**, 1802; R. F. Zhang, J. Ma, M. B. Kong, Y. S. Chen and T. S. Zhang, *Mater. Let.*, 2002, **55**, 388–393; M. L. Calzada, A. Gonzalez, R. Poyato and L. Pardo, *J. Mater. Chem.*, 1993, **13**, 1451.
6 S. P. Faure, O. Chaux and P. Gaucher, *J. Phys. IV*, 1998, **8**(Pr 9-6), 1929–37; S. P. Faure, P. Barboux, P. Gaucher and J. Livage, *J. Mater. Chem.*, 1992, **2**, 713–717.
7 L. G. Hubert-Pfalzgraf, *J. Mater. Chem.*, 2004, **14**, 3113–3123; L. G. Hubert-Pfalzgraf, *Inorg. Chem. Commun.*, 2003, **6**, 102–120, and references therein.
8 H. K. Chae, D. A. Payne, Z. Xu and L. Ma, *Chem. Mater.*, 1994, **6**, 1589–1592.
9 L. Ma and D. A. Payne, *Chem. Mater.*, 1994, **6**, 875–877.
10 (*a*) L. G. Hubert-Pfalzgraf, S. Daniele, R. Papiernik, M. C. Massiani, B. Septe, J. Vaissermann and J. C. Daran, *J. Mater. Chem.*, 1997, **7**, 753–762, and references therein; (*b*) L. Spiccia, B. O. West and Q. Zhang, *Polyhedron*, 1998, **17**, 1851–1861.
11 J. Teff, J. C. Huffman and K. G. Caulton, *Inorg. Chem.*, 1996, **35**, 2981–2987; D. J. Teff and K. G. Caulton, *Inorg. Chem.*, 1998, **37**, 2554–2562.
12 Although commercial lead 2-ethylhexanoate contains ~0.5% in weight of water, it will be written as $Pb(O_2CC_7H_{15})_2$ for clarity.
13 G. B. Deacon and R. J. Philipps, *Coord. Chem. Rev.*, 1980, **33**, 227–250.
14 J. J. Dechter, *Prog. Inorg. Chem.*, 1982, **29**, 285; R. K. Harris, J. J. Kennedy and W. McFarland, *NMR and the Periodic Table*, ed. R. K. Harris and B. E. Mann, Academic Press, New York, 1978.
15 G. D. Fallon, L. Spiccia, B. O. West and Q. Zhang, *Polyhedron*, 1997, **16**, 19–23.
16 L. Shinoni-Livny, I. P. Glusker and C. W. Bock, *Inorg. Chem.*, 1998, **37**, 1853.
17 B. A. Vaarstra, J. C. Huffman, P. S. Gradeff, L. G. Hubert-Pfalzgraf, J. C. Daran, S. Parraud, K. Yunlu and K. G. Caulton, *Inorg. Chem.*, 1990, **29**, 3126.
18 D. C. Bradley, R. C. Mehrotra, I. P. Rothwell, A. Singh, *Alkoxo and Aryloxo Derivatives of Metals*, Academic Press, London, 2001; N. Y. Turova, E. P. Turevskaya, V. G. Kessler, M. I. Yanovskaya, *The Chemistry of Metal Alkoxides*, Kluwer, London, 2002.
19 K. G. Caulton and L. G. Hubert-Pfalzgraf, *Chem. Rev.*, 1990, **90**, 969–995.
20 M. Veith and S. Mathur, *Polyhedron*, 1998, **17**, 1005–1034.
21 M. R. St, J. Foreman, M. J. Plater and J. M. S. Skakle, *J. Chem. Soc., Dalton Trans.*, 2001, 1987–1903.
22 S. Boulmaaz, R. Papiernik, L. G. Hubert-Pfalzgraf, B. Septe and J. Vaissermann, *J. Mater. Chem.*, 1997, **7**, 2053–61; L. G. Hubert-Pfalzgraf, *Polyhedron*, 1994, **13**, 1181–1195.
23 S. Daniele, L. G. Hubert-Pfalzgraf, J. C. Daran and S. Halut, *Polyhedron*, 1994, **13**, 927–932; B. Malic, I. Arcon, A. Kodrc and M. Kosev, *J. Sol–Gel Sci. Technol.*, 1999, **16**, 135–141.
24 L. Junran, H. Chunhui, L. Biaoguo, X. Guangxian and X. Gaodeng, *Huaxue Xuebao*, 1990, **11**, 226; S. T. Warzeska, M. Zonnenveld, R. van Gorkum, W. J. Muizebelt, E. Bouwman and J. Reedijk, *Prog. Org. Coat.*, 2002, **44**, 243–248.
25 B. A. Vaarstra, J. C. Huffman, W. E. Streib and K. G. Caulton, *Inorg. Chem.*, 1991, **30**, 3068–72.
26 F. Biechel, J. Dubuc and M. Henry, *New J. Chem.*, 2004, **28**, 764–69.
27 R. Papiernik, L. G. Hubert-Pfalzgraf, J. C. Daran and Y. Jeannin, *J. Chem. Soc., Chem. Commun.*, 1990, 965–66.
28 A. Altomare, M. C. Burla, M. Camalli, G. L. Cascarano, C. Giacovazzo, A. Guagliardi, A. G. G. Moliterni, G. Polidori and R. Spagn, SIR97 a program for automatic solution of crystal structures by direct methods, *J. Appl. Crystallogr.*, 1999, **32**, 115.
29 G. M. Sheldrick, *SHELXL97: Program for Crystal Structure Refinement*, University of Göttingen, Germany, 1997.
30 L. J. Farrugia, ORTEP-32 for Windows, *J. Appl. Crystallogr.*, 1997, **30**, 565.